

A systematical review of 3D printable cementitious materials

Lu, Bing; Weng, Yiwei; Li, Mingyang; Qian, Ye; Leong, Kah Fai; Tan, Ming Jen; Qian, Shunzhi

2019

Lu, B., Weng, Y., Li, M., Qian, Y., Leong, K. F., Tan, M. J., & Qian, S. (2019). A systematical review of 3D printable cementitious materials. *Construction and Building Materials*, 207, 477-490. doi:10.1016/j.conbuildmat.2019.02.144

<https://hdl.handle.net/10356/142503>

<https://doi.org/10.1016/j.conbuildmat.2019.02.144>

© 2019 Elsevier Ltd. All rights reserved. This paper was published in *Construction and Building Materials* and is made available with permission of Elsevier Ltd.

Downloaded on 09 Apr 2024 18:11:44 SGT

A Systematical Review of 3D Printable Cementitious Materials

Bing Lu ^{a, b}, Yiwei Weng ^{a, b}, Mingyang Li ^a, Ye Qian ^a, Kah Fai Leong ^a, Ming Jen Tan ^a, Shunzhi Qian ^{a, b}

a. Singapore Centre for 3D printing, School of Mechanical and Aerospace Engineering, Nanyang Technological University, 50 Nanyang Avenue, Singapore 639798, Singapore

b. School of Civil and Environmental Engineering, Nanyang Technological University, 50 Nanyang Avenue, Singapore 639798, Singapore

Abstract:

3D printing, or additive manufacturing, is a technology which adopts layer-by-layer additive deposition process to build three-dimensional objects. Over the past decade, 3D printing has been attracting more and more attention in the building and construction industry. Compared with conventional concrete casting techniques, 3D printing contributes to higher efficiency with freeform construction, greatly reduced labor and much less construction waste. However, 3D printable cementitious materials are different from conventional concrete in terms of rheology, printability, and mechanical performances. This paper aims to systematically bridge the gap between the requirement and research and development of 3D printable cementitious materials to date. Guided by 3D printing process and multi-level design of cementitious materials, the requirements for 3D printable cementitious material at different material development levels are discussed. This paper provides insights for the future development of 3D printable cementitious materials for building and construction by controlling the basic inputs of materials to obtain desired structural performance.

Key words:

3D printing, 3D printable cementitious material (3DPCM), multi-level material design (MMD), rheology, pumpability, buildability, structural performance

1. Introduction

3D printing, also known as rapid prototyping and additive manufacturing, is referred to as the process that sequentially deposits materials in a layer-by-layer manner to build expected product as per Computer-Aided Design (CAD) ^[1, 2]. In 1981, Kodama ^[3] invented the first prototype of 3D printing. Since then, the development of 3D printing has been very fast with wide applications in a number of industrial sectors, including manufacturing of complex structures and objects ^[4, 5], medical treatments ^[6] ^[7], food fabrication ^[8] and so on. The adoption of 3D printing reduces the manufacturing costs of complex objects and customized products. With further exploitations and applications, 3D printing can potentially revolutionize the manufacturing industry in the future. Recently, 3D printing has been expanded to the building and construction filed. Due to its freeform construction ability and highly automatic operation, 3D printing has distinctive advantages over conventional construction methods, contributing to higher construction efficiency, less intensive labor and less waste production ^[9-11].

As the most widely used ink of 3D printing for building and constructions, suitable 3D printable cementitious material (3DPCM) is critical to successful printing. The rest of this paper examines the development of 3DPCM as follows: general 3D printing processes of cementitious material are

introduced through various printing systems in Section 2, where the fresh performance requirements of 3DPCM are also specified. To guide the review work and potential future material development in a systematical way, multi-level material design (MMD) approach is proposed for 3DPCM in Section 3 considering material related properties/performance at different levels, then the paper follows the proposed MMD approach to review and analyze the key parameters in developing 3DPCM. This review work covers multiple levels including mixture design, printing-related material properties and structural performance of 3DPCM in Sections 4 to 6 respectively, which are expected to provide insights for future design and exploitation of 3DPCM for intended structural performance.

2. 3D Cementitious Material Printing Systems

2.1 Gantry-based 3D cementitious material printing system

Contour Crafting is the first gantry-based large-scale 3D cementitious material printing system. It fabricates objects with smooth surfaces by computer-controlled gantry crane, which is of high efficiency and accuracy ^[12]. In the printing process, the cement-based paste is extruded successively through the nozzle to form the rim of expected structure. A layer is printed when the nozzle moves back to its origin and forms a closed region. Then the nozzle lifts up to start printing another layer atop the previous layers. With the scraping by top and side trowels, the printed structure has a smooth surface, as can be seen in Fig. 1 (a). Materials such as conventional concrete can then be poured into this closed section to form a composite structure if needed (see Fig. 1 (b)) ^[13]. In this case, Contour Crafting creates 3D printed permanent formworks, which will be part of the printed structure.

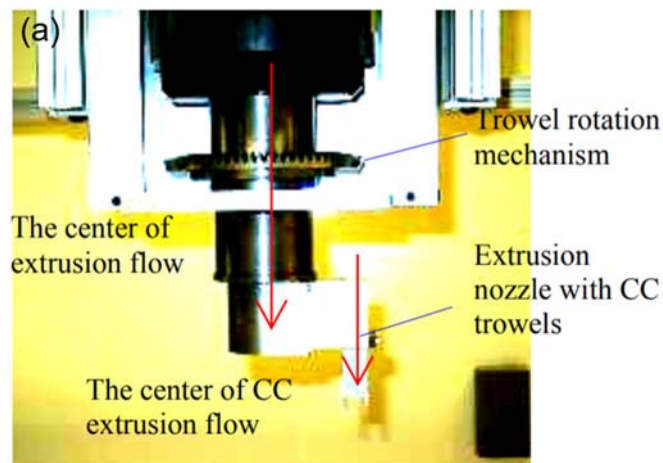




Fig. 1 Contour Crafting^[13]: (a) schematic drawing of printing nozzle; (b) formation of composite structure. Reproduced from Ref. [13] with permission from IAARC.

Concrete Printing developed by Lim et al.^[14] is also based on the extrusion process of cementitious materials. Compared with Contour Crafting, it has better printing system control and higher printing resolution^[14]. The printing system contains a giant frame mounted with movable beam and nozzle (See Fig. 2 (a)). The nozzle moves along the beam while the beam moves in the other two orthogonal directions to implement free-form 3D printing^[15, 16]. Compared with Contour Crafting, layered texture can be clearly observed due to the lack of surface scraping in Concrete Printing (See Fig. 2 (b)). However, the dimensions of filaments are much smaller than Contour Crafting. Thus, the pixels of the printed concrete surface are very small. The layered texture also exists in the structures printed by similar gantry-based printing system^[17].

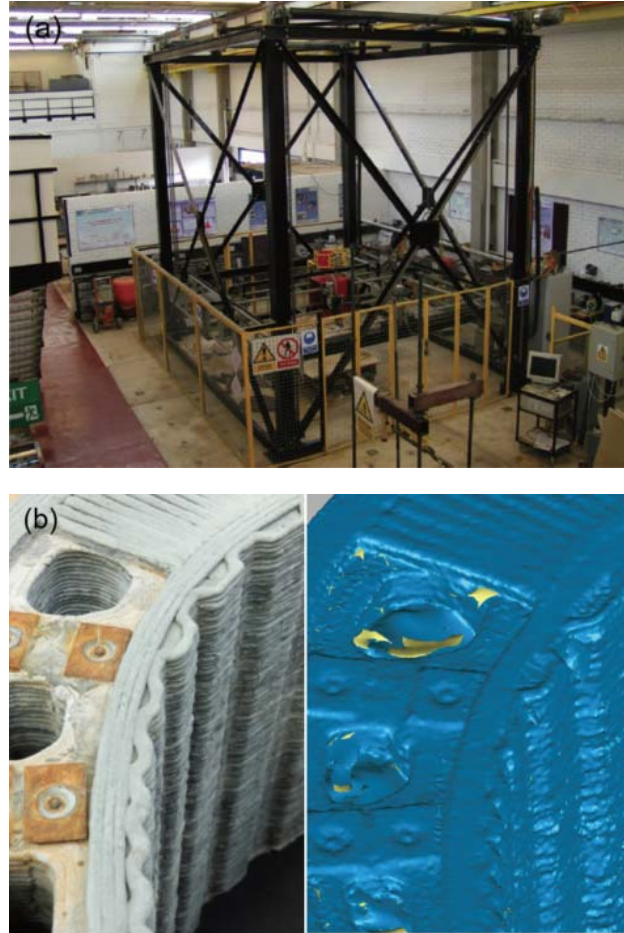


Fig. 2 Concrete Printing ^[16, 17]: (a) gantry framework; (b) details of printed structure and scanned surface; (c) layered texture in printed structure by similar gantry-based printing system. Fig. 2 (a) and Fig. 2 (b) are reproduced from Ref. [16] with permission from IAARC.

2.2 Robot-based 3D cementitious material printing system

In robot-based 3D cementitious material printing system, robot is used to control the movement of printing nozzle as per programmed path ^[18, 19]. Fig. 3 illustrates the equipment of a robotic arm printing system for large-scale 3D cementitious material printing ^[19]. The raw ingredients of cementitious material are mixed and then the fresh material is delivered to the nozzle for printing. At the same time, the robotic arm moves with the mounted nozzle to implement the layer-by-layer 3D printing process. Compared with the gantry-based 3D cementitious material printing system, the robot-based 3D cementitious material printing system has less size limitations on the designed structure. On the other hand, the robot-based 3D cementitious material printing system is mounted on a movable platform, which is suitable for onsite printing. Moreover, the collaborative printing by synchronized robots further reduces the size and location limitations of 3D cementitious material printing ^[19].

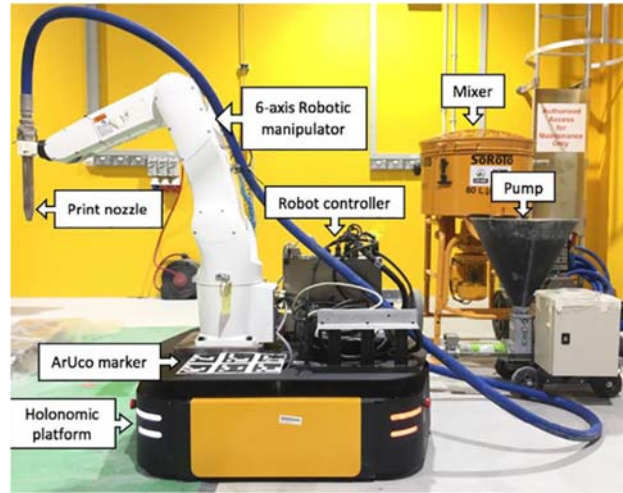


Fig. 3 Robotic arm printing system for large-scale 3D cementitious material printing ^[19]. Reproduced from Ref. [19] with permission © Elsevier.

In addition to the aforementioned major cementitious material printing systems, there are some other similar printing systems, e.g., computer-controlled crane with slewing structures ^[20], binder-jetting 3D printing with cement paste penetration ^[21]. From the introduction of different 3D cementitious material printing systems, it can be found that the printing process can be divided into two successive phases. In the first phase, which can be referred to as delivery phase, 3DPCM is prepared and delivered through the hose to the printing nozzle. In the second phase, which can be referred to as deposition phase, the material is extruded from the moving nozzle and laid atop the supporting platform or printed layers. It should be noted that among the practices reported in the literature, the delivery phase could be slightly different based on the type of material preparation. Some printing systems deal with premix 3DPCM, where the material is only prepared at the beginning of the printing. In contrast, the other printing systems require continuous mixing and preparation of 3DPCM during the printing process. The two categories could also be referred to as off-line mixing and in-line mixing ^[22] respectively. The different time span from mixing to printing in these two types of material preparation could significantly affect the performance of 3DPCM.

The core equipment in the delivery phase is pump, while the core equipment in the deposition phase is the end effector to control the movement of the nozzle. Based on different operation mechanisms, direct-acting piston pump ^[23], peristaltic squeeze pump ^[23] and screw pump ^[24] could be applied to deliver the material. With the triggered pressure difference in the hose, the material is forced to move to the printing nozzle and be extruded out. On the other hand, different end effectors contribute to the above different types of printing systems, whether it is associated with gantry, robot, etc.

The printing process requires specific fresh properties for cementitious materials. In the delivery phase, the material should be easy to deliver to the nozzle without causing blockage, which requires good pumpability of the material ^[25]. In the deposition phase, the printed material should have little deformation to ensure sufficient support for successive layers. This requirement of little deformation of the printed layer can be labeled as buildability ^[26]. Therefore, the material needs to have good buildability in the deposition phase. To summarize, suitable 3DPCM should possess good pumpability for delivery and good buildability for deposition in 3D printing process.

3. Multi-level Material Design

To systematically capture some of the significant factors in the design of 3DPCMs, the multi-level material design (MMD) is proposed and illustrated in Fig. 4. It covers the design span from raw ingredients to ultimate structural performance. The three pyramids of MMD are corresponding to the three consecutive stages in the design of 3DPCM, i.e. mixture design, printing process and composite structure. These pyramids are linked together by two common apexes. For each pyramid, the factors at the lower three apexes largely influence the properties/performance at upper apex, which in turn significantly impacts the properties/performance at a higher level together with other two factors. The proposed MMD makes the initial attempt to explain the contribution of these significant factors in the material design span. In addition, it gives the insight for future improvement on systematical and standardized designs of 3DPCMs.

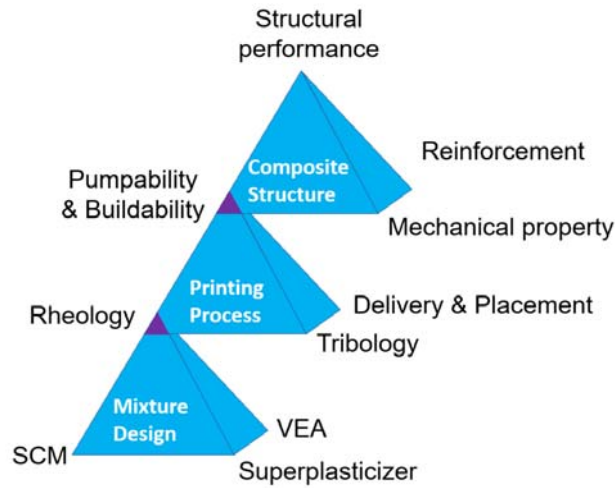


Fig. 4 Multi-level material design for 3DPCM

At the lowest level (i.e., the lowest pyramid), different raw ingredients of mixture design, including supplementary cementitious materials (SCM), superplasticizer and viscosity enhancement agent (VEA) contribute to the rheological properties of the material. Rheology describes the deformation and flow characteristics of the material [27], which affects the pumpability and buildability of the printing process. In addition to rheology, pumpability and buildability are also influenced by equipment-related parameters, such as tribology, delivery and placement with different pumping facilities. These are reflected in the intermediate level, i.e., the middle pyramid. As an input to the highest level (i.e., the highest pyramid), pumpability and buildability contribute to the structural performance with other inputs from mechanical property and reinforcement. As 3D cementitious material printing is a very comprehensive topic, organizing the content according to this multi-level material design concept can sharpen the focus of our review work such that the key developments in 3DPCM can be captured.

4. Influence of Material Composition on the Rheological Properties of 3D Printable Cementitious Materials

In the current 3D cementitious material printing, due to size limitation of the delivery system, coarse aggregate (e.g. particle size larger than 2 mm ^[28]) typically is not used in the mix design. In this case, 3DPCMs are usually mortars ^[20, 29], instead of concretes. The 3D printing process is a flowing process. The materials are flowing in the pipe during pumping and extruded out of the nozzle. Thus, rheology of the materials is of critical importance.

The most common way to describe the flowability of cementitious materials is to obtain the equilibrium flow curve. It is the relationship between equilibrium shear stress and shear rate. Commonly, the equilibrium shear stress is obtained by applying a constant shear rate. The shear stress would increase to a peak value, and then decay till reaching equilibrium value ^[30, 31], as shown in Fig. 5. The equilibrium shear stress value and the corresponding shear rate is plotted in Fig. 6.

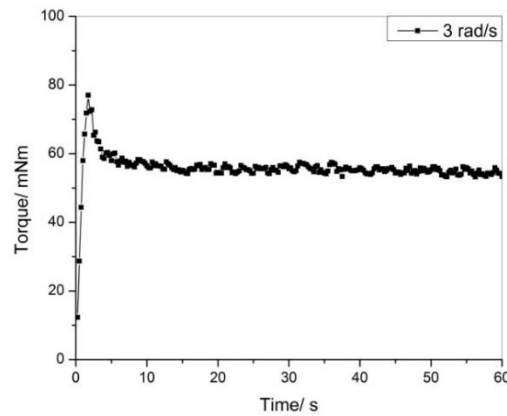


Fig. 5 Stress development under constant shear rate ^[31]. Reproduced from Ref. [31] with permission © Elsevier.

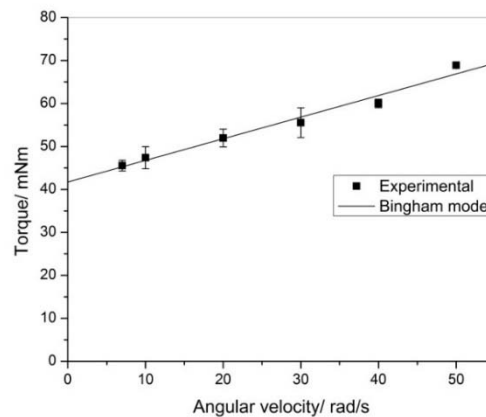


Fig. 6 The equilibrium flow curve of mortar ^[31]. Reproduced from Ref. [31] with permission © Elsevier.

It could be seen that for mortars, there is a linear relationship between equilibrium shear stress and shear rate. Thus, the most frequently applied viscosity model is Bingham Plastic model [32]. Bingham Plastic model depicts a linear relationship between shear stress τ (Pa) and shear rate ($d\gamma/dt$) (1/s), as shown below:

$$\tau = \tau_0 + k \frac{d\gamma}{dt} \quad (1)$$

where τ_0 (Pa) is referred to as dynamic yield stress, representing the minimum stress needed to maintain flow; k (Pa·s) is referred to as plastic viscosity, representing the stress increment for unit increment of shear rate once dynamic yield stress is exceeded. These two parameters are basic rheological parameters describing the flowability of cementitious materials.

Recent studies [33-35] also reveal that there exists another yield stress, which is higher than dynamic yield stress. It is believed to be the yield stress corresponding to the flocculation state before the microstructure is broken down, which is referred to as static yield stress. With the measurement of static yield stress, the structural build-up of cementitious materials can be effectively monitored [35]. The information of structural build-up is useful for the buildability assessment [36], which further relates to the structural performance of 3DPCM.

Thus, the rheological parameters of cementitious materials are subjected to the change in mix proportions and time. Early hydrates are formed during the early hydration period, which is usually within 20 mins after the contact between water and cement. In considering the sustainability of the cement industry, supplementary cementitious materials (SCM) are commonly used to replace cement paste. These mineral replacements have different mineral components than cement and hydration rates, thus modifying the early rheological parameters [37, 38]. In the meanwhile, superplasticizers are commonly used as water reducing agent in modern concrete. They usually adsorb on the surface of cement particles/agglomerates and reduce attractive bonding between particles/agglomerates, thus increasing flowability [39]. It helps to reduce water content and increase the mechanical strength of cementitious materials. For example, pumping of self-consolidating concrete (SCC) requires high flowability. Likewise, in 3D printing, to guaranty the continuous pumping process and prevent clogging, superplasticizers should be added to enhance flowability and pumpability. Furthermore, after pumping and extrusion out of the nozzle, the 3D printable materials are supposed to be strong enough to support its own weight and further layers above; and stiff enough to keep its shape. Cementitious materials become stronger and stiffer over time due to cement hydration. The consumption of water and reaction to form hydrates, such as C-S-H, C-H and CaCO_3 make the materials stronger and stiffer [36, 40]. However, for the usual application of 3D printing, the whole printing period occurs within 2 hours and thought to be dormant period [23]. Some accelerators could increase hydration and shorten the dormant period. Certain types of viscosity enhancement agents (VEA), such as nanoclay [33, 41], could enhance the green strength and static yield stress of materials.

It could be seen that for successful 3D printable materials, it has bi-fold rheological properties. On one hand, the materials should be flowable enough to be pumped and extruded; on the other hand, the materials should be strong and stiff enough to maintain its shape and sustain the weight of its own and the layers above. From the perspectives of rheology, it should have low dynamic yield stress and high

static yield stress. According to Qian and Kawashima ^[31], the discrepancy between dynamic and static yield stress is related to thixotropy. Thus, the 3D printable materials should have high thixotropy, as has been discussed by pervious researchers ^[17, 29].

4.1 Supplementary cementitious materials (SCM)

The most widely-applied supplementary cementitious materials are fly ash, ground blast furnace slag and silica fume. All of them contains mineral components and can be triggered to have secondary hydration in the cement hydration process, which are commonly referred to as pozzolanic reaction. As mentioned at the beginning of this section, the incorporation of these SCM can contribute to different rheological behaviors.

There are many experimental studies and theoretical analyses to investigate the rheological effects of SCM incorporation. Jiao et al. ^[42] have summarized the rheological effects from literature to draft the corresponding rheographs. From these rheographs, Jiao et al. found that there are some contradictory reports. However, some general conclusions could still be drawn, which can be useful to instruct the design of 3DPCM. In the cases of fly ash, the rheological effects vary a lot among different reports, but class F fly ash can significantly decrease plastic viscosity compared with class C fly ash ^[42]. In the most cases, plastic viscosity is reduced with the increasing dosage of ground blast furnace slag, while yield stress varies due to the competition of prominent micro-filling effect and increased water demand from high specific area. Most reports point out that the increase of silica fume contribute to higher dynamic yield stress and higher plastic viscosity, and the effects are highly associated with the water binder ratio and different types of superplasticizer applied ^[42].

Rheological behavior in ternary blends system has also been investigated in details ^[42]. The reports show that the yield stress is dominated by the particle size distribution of these raw ingredients, e.g. addition of cementitious material which has an intermediate particle size distribution between cement and silica fume can lead to the decrease of yield stress. For ternary blends system of cement, fly ash and ground blast furnace slag, both yield stress and plastic viscosity were reported increased ^[43]. In this case, 20% fly ash with 40% slag combination showed the highest increase in plastic viscosity ^[44].

4.2 Superplasticizer

Generally, superplasticizer can be classified into such types: purified lignosulfonates, carboxylate synthetic polymers, sulfonated synthetic polymers and synthetic polymers with mixed functionality ^[45, 46]. As the superplasticizer is used to improve the workability of mortar or concrete materials, its addition decreases yield stress and plastic viscosity, which has been verified by many rheological experiments ^[40] ^[47]. However, there exist critical and saturation dosages for the superplasticizer specifically. Below the critical dosage (too little amount) or above the saturation dosage (too much amount), superplasticizer has minimal effects on the rheological behavior ^[48]. The critical and saturation dosages are dependent on the molecular structure of the superplasticizer, e.g. polycarboxylate and polyphosphonate-based superplasticizer have lower dosage than naphthalene and melamine-based superplasticizer ^[45].

The rheological effects of superplasticizer are also hinged on the water binder ratio of the material. For the material with high water to cement ratio, there are minimal differences in rheological influence between different superplasticizers. However, in the case of low water to cement ratio such as 0.20, the polynaphthalene sulfonate polymer-based superplasticizer is ineffective to change the rheological properties of the material, while different polycarboxylic ether type superplasticizer shows different extents of reducing rheological parameters [48, 49].

Research studies pointed out that the effectiveness of superplasticizer in rheological changes is highly dependent on its type, e.g. polycarboxylate-based superplasticizer shows a stronger reduction of plastic viscosity but weaker reduction of yield stress compared with naphthalene sulphonate-based superplasticizer [42]. Different types of superplasticizer have different molecular structures, which can account for different efficiency of altering rheological properties, e.g. naphthalene sulfonate formaldehyde polycondensate superplasticizer has a linear structure and reduces the attraction of particles by electrostatic repulsion; polycarboxylic ether superplasticizer has a comb-like structure and reduces the attraction of particles by steric hinderance [48, 50]. Research studies also reported that low side chain density of the superplasticizer contributes to the reduction of yield stress, and the rheological changes brought by effective superplasticizer can be very sensitive to the dosage [48].

The type of superplasticizer also has impacts on the robustness of rheological effects, which is linked to its compatibility with different cement systems. Lack of robustness and compatibility lead to great rheological changes with small dosage variation, time and possible segregation [45], e.g. polysulfonate-based and polycarboxylate-based superplasticizer possess good compatibility with high alkali and sulphate cement, while polysulfonate-based superplasticizer has poor compatibility with low alkali cement.

4.3 Viscosity Enhancement Agent

Viscosity Enhancement Agent (VEA) is frequently applied to enhance the fluidity and cohesion of fresh concrete materials, leading to improved robustness [51, 52]. For concrete materials, the addition of VEA can effectively influence the rheological behaviors. The applied shear stress has a certain influence on the rheological behavior of concrete materials incorporating VEA. It has been reported that while some material exhibited shear thinning behavior when subjected to high shear stress, it exhibited the opposite trend when subjected to low shear stress [52].

Similar to superplasticizer, the rheological effectiveness of VEA also depends on its type. Research studies have shown that hydroxypropyl methyl cellulose-based VEA reduces yield stress but increases plastic viscosity [47]; polysaccharide-based VEA significantly increases yield stress, while microsilica-based VEA induces low plastic viscosity [53]. In addition, nanoclay-based VEA can significantly increase static yield stress and enhance thixotropic property of the material [33, 54], which further improves the shape stability of the material [54, 55]. It has also been found that the combination of nanoclay and PCE superplasticizer could obtain a cementitious mixture with low dynamic yield stress, yet high thixotropy and high static yield stress [56].

5. Pumpability and Buildability of 3D Printable Cementitious Materials

From the analysis of 3D cementitious material printing process, it is revealed that 3DPCM should possess good pumpability for delivery and good buildability for deposition. Materials with good pumpability can be easily delivered through the hose to the printing nozzle with low risk of blockage. The blockage in the printing process leads to discontinuity of the extruded material and further impaired structural performance of 3DPCM. Thus, the adoption of material with good pumpability improves the robustness of 3D printing by reducing the risk of blockage. Materials with good buildability can build up to large height with negligible deformation, which ensures the consistency of printed dimensions and structural stability. As mentioned in Section 4, successful 3DPCMs should have bi-fold rheological requirements. In addition to the analysis of rheology, tribology and placement/delivery of the material should also be taken into consideration, which exerts import influence on the printing process. This part of review and analysis covers the second pyramid in the multi-level material design illustrated in Fig. 4.

5.1 Analysis of rheology

As rheology describes the flow characteristics of the material, it is necessary to analyze how rheological parameters affect the pumpability and buildability of 3DPCM respectively. Pumpability can be assessed by shear viscosity of the material in the hose^[57]. Considering Bingham Plastic model, shear viscosity μ (Pa·s) is calculated as follows:

$$\mu = \frac{\tau}{d\gamma/dt} = \frac{\tau_0}{d\gamma/dt} + k \quad (2)$$

With constant equipment-related control such as adoption of the same pipeline system and constant flow rate, shear viscosity or the consequent pressure drop can be the indicator for pumpability. The flow of cementitious material inside the hose follows plug flow when the flow rate is small^[58], of which flow velocity profile and shear stress distribution are shown in Fig. 7.

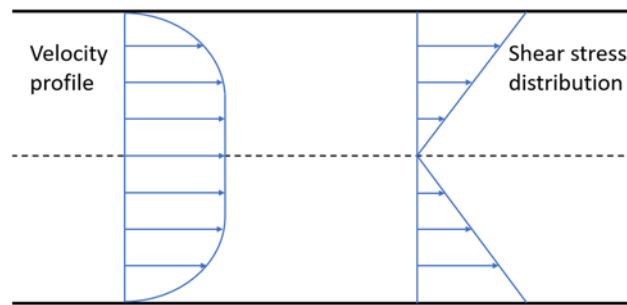


Fig. 7 Flow velocity and shear stress distribution of cement mortar material inside the hose

The flow rate of the material Q (m³/s) can be expressed in the form of pressure drop $\Delta p/L$ (Pa/m), dimensions of the hose (radius R (m) and length L (m)) and rheological parameters (yield stress τ_0 (Pa) and plastic viscosity k (Pa·s))^[58], namely

$$Q = \frac{\pi R^4}{8k} \left(\frac{\Delta p}{L} \right) \left(1 - \frac{4}{3} \phi + \frac{1}{3} \phi^4 \right) \quad (3)$$

$$\phi = \frac{\tau_0}{\tau_w} = \left(\frac{L}{\Delta p} \right) \frac{2\tau_0}{R} \leq 1 \quad (4)$$

where τ_w (Pa) is the shear stress at the wall of the hose, which is not smaller than yield stress τ_0 . It is revealed that lower dynamic yield stress and lower plastic viscosity contribute to smaller pressure drop with the same flow rate, indicating better pumpability of the material. Hence, lower rheological parameters are desirable in the delivery phase.

Kaplan derived corresponding equations to describe the flow behavior of cementitious materials inside the hose for large flow rate, which involves viscous flow apart from plug flow^[59]. The influence of the lubricating layer formed by the material was also considered in the calculations. From the calculations, the same conclusion was proposed, i.e. lower plastic viscosity and dynamic yield stress contribute to better pumpability. Therefore, the conclusion is applicable to cementitious material in any flow rate.

When the material is extruded from the nozzle to form filaments, good buildability is required. Buildability is heavily influenced by the deformation behavior of extruded filaments under gravity. The most direct way to assess buildability is to compare the maximum height or number of layers that can be built with the same printing setup. Negligible deformation is required for 3DPCMs. Buildability can also be quantitatively assessed by the green strength of the material. Green strength refers to the maximum stress that the material can withstand in the fresh state^[24, 60]. Judged by its definition, high green strength increases the ultimate pressure the printed filaments can resist. In the literature^[61, 62], slump value is frequently used as an indirect assessment of buildability. To minimize the deformation of the printed layer, zero slump value is specified for 3DPCMs. To summarize, little slump value or high green strength suggests better buildability of the material.

Khoshnevis et al.^[62] have analyzed the deformation of the printed sulfur concrete filament with rectangular cross section. The analysis depicts the relationship between slump value and rheological parameters. As the deformation analysis does not involve material information of sulfur concrete, it can be applied to all the extrusion-based 3DPCMs. The slump value S (m) can be expressed by the following equation:

$$S = H - \frac{2\tau_s}{\rho g_0} \left[1 + \ln \left(\frac{\rho g_0 H}{2\tau_s} \right) \right] \quad (5)$$

where H (m) is the original height of the printed filaments, ρ (kg/m³) is the fresh density of printed material, and g_0 (m/s²) is gravitational acceleration. τ_s is the static yield stress as the material flocculates and recovers the microstructure after it is extruded.

Eq. (5) reveals that high static yield stress and low density contribute to low slump value, indicating better buildability. Specifically, if the ratio of static yield stress to fresh density is large enough, there will be no slump for the concrete material. A similar conclusion can be obtained through the calculation of green strength. In the critical case where there is no slump value exactly (i.e. $S = 0$), green strength σ_{gr} can be expressed as:

$$\sigma_{gr} = \rho g_0 H = 2\tau_s \quad (6)$$

And the theoretical maximum height H_{max} (m) and number of layers the material can build without

deformation n_{\max} are:

$$H_{\max} = \frac{2\tau_s}{\rho g_0} \quad (7)$$

$$n_{\max} = \frac{2\tau_s}{\rho g_0 h_0} \quad (8)$$

where h_0 is the height of each printed layer. Hence, for better buildability of 3DPCM, high static yield stress and low density are desired.

Perrot et al. have constructed a more general model to link green strength with static yield stress [36]. The model considers the geometric influence of printed structure and evolution of static yield stress, and in this case, green strength is expressed as:

$$\sigma_{gr} = \alpha_{geom} \tau_s(t) \quad (9)$$

where α_{geom} is the geometric factor and $\tau_s(t)$ is the static yield stress considering time effect. The geometric factor α_{geom} varies for different printed structures, e.g. for a hollowed cylinder which is one of the common structures in 3D cementitious material printing, the geometric factor α_{geom} can be computed as follows [24]:

$$\alpha_{geom} = (R_2^2 - R_1^2)^{-1} \left(\frac{1}{2} + \frac{C_\alpha}{R_2^2} \right)^{-1} \sqrt{\frac{3}{4} + \frac{C_\alpha^2}{R_2^4}} \left\{ \frac{4}{H} \left[\frac{(R_2^3 - R_1^3)}{6} + C_\alpha (R_2 - R_1) \right] + 2C_\alpha \left(\sqrt{\frac{3R_2^4}{4C_\alpha^2} + 1} - \sqrt{\frac{3R_1^4}{4C_\alpha^2} + 1} \right) \right. \\ \left. - 2C_\alpha \left[\operatorname{arcsinh} \left(\frac{2C_\alpha}{\sqrt{3}R_2^2} \right) - \operatorname{arcsinh} \left(\frac{2C_\alpha}{\sqrt{3}R_1^2} \right) \right] - 2R_1^2 \left(\frac{3}{4} + \frac{C_\alpha^2}{R_1^4} \right)^{-1/2} \left(\frac{1}{4} - \frac{C_\alpha^2}{R_1^4} \right) - 2R_2^2 \left(\frac{3}{4} + \frac{C_\alpha^2}{R_2^4} \right)^{-1/2} \left(\frac{1}{4} - \frac{C_\alpha^2}{R_2^4} \right) \right\} \quad (10)$$

where R_1 and R_2 are the inner radius and outer radius respectively. C_α in Eq. (10) can be determined by the following equation:

$$\frac{\frac{1}{2} - \frac{C_\alpha}{R_2^2}}{\sqrt{\frac{3}{4} + \frac{C_\alpha^2}{R_2^4}}} - \frac{\frac{1}{2} - \frac{C_\alpha}{R_1^2}}{\sqrt{\frac{3}{4} + \frac{C_\alpha^2}{R_1^4}}} + \operatorname{arcsinh} \left(\frac{2C_\alpha}{\sqrt{3}R_2^2} \right) - \operatorname{arcsinh} \left(\frac{2C_\alpha}{\sqrt{3}R_1^2} \right) = 0 \quad (11)$$

Based on the proposed model, it is accessible to estimate the failure height of the printed structure.

Experimental studies of buildability of 3DPCMs have been reported by several researchers, which can offer verifications for the proposed models. Le et al. [63] have conducted printing tests for different 3DPCMs, and their results show that higher yield stress contributes to more layers that the material can build (see Fig. 8). The same conclusion has been reported by Weng et al. [24]. Voigt et al. [55] have reported that increasing the content of fiber and clay materials such as metakaolin lead to higher green strength, while increasing the content of fly ash makes the material easier to flow. Increasing sand-binder ratio [63], the addition of polymer resin or thickening agents [64] can lead to smaller deformation of printed structures, indicating better buildability. These results can be explained by their rheological effects, which indirectly verify the theoretical analysis.

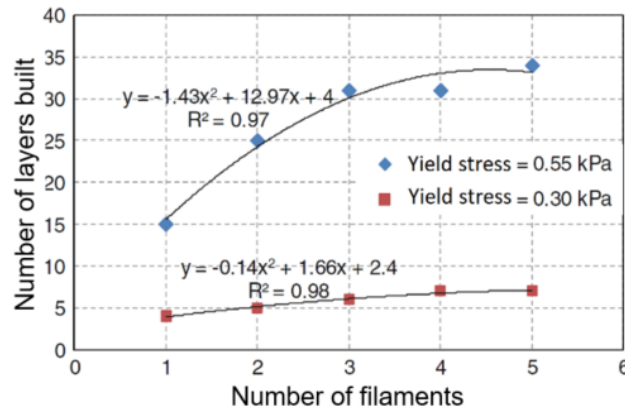


Fig. 8 Buildability results of 3DPCMs with different yield stress ^[63]. Reproduced from Ref. [63] with permission © RILEM.

The analysis of rheology indicates different rheological requirements for 3DPCMs in the delivery and deposition phase. In the delivery phase, the material should possess low plastic viscosity and low dynamic yield stress for better pumpability; in the deposition phase, the material should possess high static yield stress for better buildability. The paradox could be more significant in the printing with off-line mixing. The prepared 3DPCM undergoes more time before delivery compared with the in-line mixing, while generally the yield stress increases with the hydration of the fresh material ^[36]. To meet seemingly conflicting rheological requirements in different phases, tailoring rheological properties with the consideration in the first pyramid is required.

There could be three strategies in the rheological tailoring. As the deposition phase is after the delivery phase, one of the tailoring strategies is to utilize time-dependent rheological behavior. Special raw ingredients or additives such as accelerator can be added to the mix to trigger the great increase of yield stress over time. However, the excessively rapid rising of yield stress may lead to poor pumpability or even clogging of hose. In this case, open time is critical to the printing performance of material ^[63] ^[65], which identifies the window available for printing. The insight for the second strategy comes from the influence of delivery on buildability. This strategy is to decrease rheological parameters for better pumpability and recover them after the material is printed. The strategy requires large compressibility of the material. In the pumping process, the material with high compressibility is compacted under pressure, which triggers the rheological change. The detailed mechanism will be introduced in Section 5.3. The third strategy is to make compromises in both phases. The material can be designed to have high static yield stress and low fresh density for good buildability as well as low plastic viscosity for better pumpability. Adjusting the raw ingredients or additives, e.g., increasing silica fume/cement ratio can contribute to the desired rheological properties. More information of the rheological effects of different raw ingredients of concrete materials can be found in Section 4. To reduce the fresh density of the material, lightweight aggregates may be adopted in the mix design.

Several experimental studies on the evolution of rheological parameters related to printing have been reported, while most of them focus on yield stress evolution. Yield stress evolution of 3DPCMs containing different supplementary cementitious materials has been investigated ^[40, 66]. Cementitious materials containing metakaolin and Class C fly ash have a significant increase in yield stress with time ^[66]. However, no clear trend on the yield stress can be observed for other supplementary cementitious

materials. On the other hand, yield stress evolution of 3DPCMs incorporating different additives has also been investigated [36, 63]. In Le et al.'s work [63], shear vane apparatus was adopted to assess the shear strength of the material, which is regarded as yield stress in the analysis. Fig. 9 shows the evolution of yield stress (shear strength) of the material with different dosages of superplasticizer and retarder. The figures reveal that increasing dosage of superplasticizer can effectively extend the window of workable yield stress for printing. In this case, the window ranges from 0.3 to 0.9 kPa. In comparison, increasing dosage of retarder does not have consistent effects.

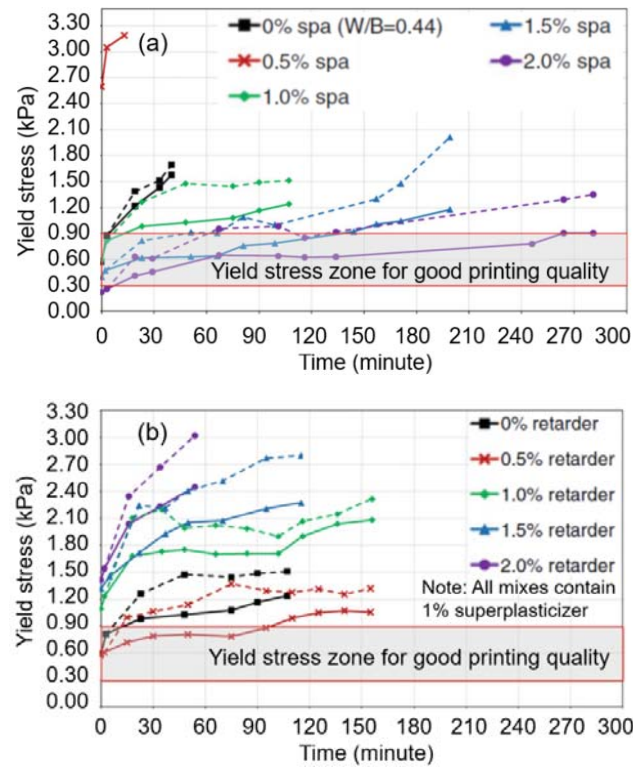


Fig. 9 Yield stress (shear strength) evolution [63] under: (a) different dosage of superplasticizer; (b) different dosage of retarder (solid curves for agitated samples; dotted curves for non-agitated samples).

Reproduced from Ref. [63] with permission © RILEM.

The evolution of rheological parameters has also been investigated with different rapid hardening ingredients. Khalil et al. [67] reported the adoption of calcium sulfoaluminate (CSA) cement for 3D printing. By replacing 7% of ordinary Portland cement with CSA cement, yield stress increases rapidly with time. Kim et al. [68] found that increasing the ratio of calcium aluminate cement (CAC) to ordinary Portland cement leads to rapid development of viscosity. Similar rheological results can be found for material incorporating rapid hardening ingredient such as Magnesium Potassium phosphate cement [69]. In addition, through the application of appropriate accelerating agents, rapid setting and hardening can be achieved in several minutes [70], which also leads to the rapid increase of rheological parameters.

5.2 Analysis of tribology

In addition to rheology, tribology of the material should be taken into consideration when the

material flows in the hose. There are two types of friction in the delivery phase: (a) internal friction of the material which contributes to rheology^[58], and (b) friction between the material and the wall of the hose. Correspondingly, there exist two types of blockage in concrete material pumping^[23, 71]. In the first type, a mass of concrete material cannot be pumped to move inside the hose under certain pumping pressure. This is due to the high internal friction brought by high rheological parameters, which has been clarified in Section 5.1. In the second type of blockage, water dissipates from the mix under pressure with solid material left behind to cause clogging of the hose.

The second type of blockage is related to the segregation of material under pressure. In the delivery phase, water transmits the pumping pressure to other ingredients^[23]. If the lowest pumping pressure to initiate flow (pumping pressure threshold) is higher than segregation pressure, the pressure-induced segregation happens^[72]. The segregation leads to the loss of material homogeneity and water is squeezed out from the material. To prevent the second type of blockage, it is critical to prevent severe segregation in the delivery phase. Assaad et al.^[73] have investigated the relationship between segregation index and rheological parameters, which is shown in Fig. 10. The figure reveals that reducing flow resistance or torque viscosity increases segregation index. In other words, decreasing yield stress or viscosity increases segregation tendency. Hence in the material design, both viscosity and yield stress should have minimum design values, which can be examined through column segregation tests, pressure bleeding test or similar experiments.

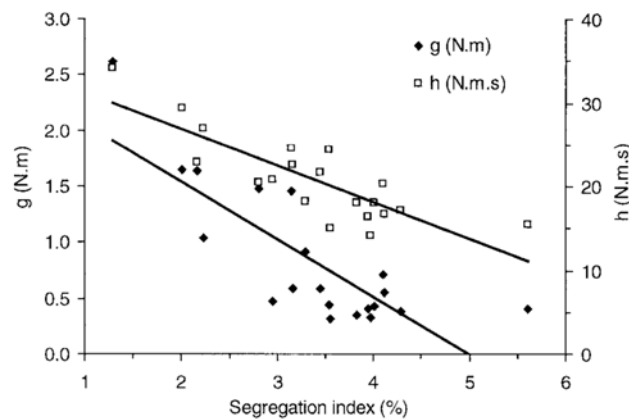


Fig. 10 Relationship between segregation index and rheological parameters^[73]. Reproduced with permission from Ref. [73] © American Concrete Institute.

The tribological analysis can be verified through concrete pumping practices. Increasing cement content can increase the resistance to segregation when the concrete material is pumped^[74]. Incorporating more fine particles also reduces the risk of segregation in the pumping process^[23]. The mechanism of these practices in controlling segregation in the pumping process can be attributed to higher rheological parameters of the material^[40].

Based on the above discussions, a schematic diagram shows different combinations of yield stress and plastic viscosity in relation to printing, as can be shown in Fig. 11. In total, there are five regions in Fig. 11. The descending curve sets apart Regions 1, 2 and Regions 3, 4 as the material with good and poor pumpability respectively. The curve is drawn based on the discussion of Eq. (3). In Eq. (3), all the

equipment-related parameters and flow rate are kept the same. The dashed line sets apart the material with good and poor buildability, which is related to Eq. (7). Very low yield stress or plastic viscosity can lead to segregation of the material, which is denoted as Region 5.

The previous discussions on rheological tailoring strategies in Section 5.1 can be further extended based on Fig. 11 correspondingly. The first and second strategies are to design the material with rheological parameters in Region 2 for good pumpability, then bring its rheological parameters to Region 1 and Region 3 in the printing phase for good buildability. The third strategy is to deliberately tailor the rheological parameters of the material from Regions 2 or 3 to Region 1. Special additives may be added to the mixture to elongate open time for this strategy.

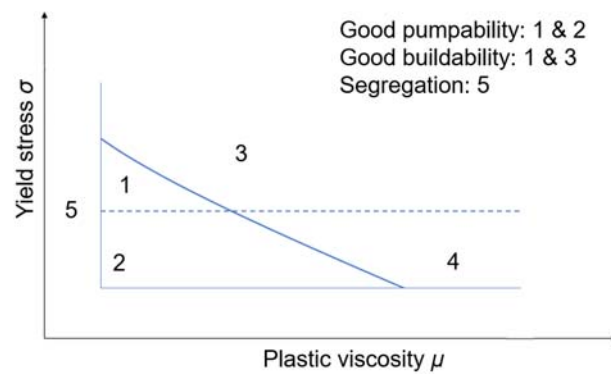


Fig. 11 Schematic diagram showing different combinations of yield stress and plastic viscosity in relation to printing

5.3 Delivery and placement

In 3D cementitious material printing, delivery greatly affects pumpability and buildability of the material. Regarding Eq. (3), increasing the radius of the hose, reducing the total pipe length can lower pumping pressure required for the material. Material with higher rheological parameters yet the same pumpability can be developed accordingly. Additional air pressure can be added to push the material forward, which has been applied by Keating et al. [75] in their 3D printing of foam concrete material, as can be seen in Fig. 12. To overcome friction in the delivery phase, 3DPCM is compacted under pumping pressure. The compaction of the material leads to higher fresh density and higher yield stress [76]. Therefore, buildability of the material is affected by such compaction in the delivery phase. This process-induced effect is critical to materials with large compressibility, e.g. air-entrained concrete materials.



Fig. 12 3D printing of foam concrete materials^[75]. Reproduced from Ref. [75] with permission © American Association for the Advancement of Science.

The compaction of the material in the delivery hose offers a tailoring strategy for 3DPCMs. This strategy was previously applied in developing sprayable concrete materials, and the corresponding rheological change is referred to as slump-killing effect^[77]. For material with high yield stress, extra air-entraining agent can be added to decrease the rheological parameters for better pumpability^[40, 47]. When the material is printed, higher yield stress caused by the compaction will contribute to better buildability.

Placement of the material also affects the measured buildability. As suggested in Fig. 8, printed layer with a wider width, e.g. more parallel filaments lead to a larger number of layers built. It may be attributed to the stability of the printed structures. Small disturbance can lead to the offset of printed layers in the printing process, and the printed structure with narrow layer width is more susceptible to the offset moment. On the other hand, different structures have different geometric factors as described in Eq. (9), which certainly affect the maximum printable height. Elastic buckling may happen before the printed material reaches the critical yield stress of plastic collapse^[78], e.g. the wall structure with a large height to width ratio may bend over in the printing. This situation also limits the maximum height of the printed structure. Detailed theoretical analysis, simulations or experiments need to be carried to decide whether plastic collapse or elastic buckling dominates the final failure^[29, 78]. For large-scale 3D cementitious material printing such as garden villas^[79], the printing duration is significantly longer than the dormant period of cement hydration. In this case, the evolution of rheological parameters contributes to higher buildability, especially for the material in the bottom layers.

6. Structural Performance of 3D Printable Cementitious Materials

The structural performance of conventional concrete materials is largely governed by its mechanical property and the reinforcement in the structure, which is also applicable for 3DPCMs given that process difference between casting and 3D printing is adequately considered. Obviously, the layer-by-layer printing process greatly affects the mechanical property and subsequently structural performance of 3DPCMs. Furthermore, the very different methods of reinforcement addition in 3D printing could significantly impact structural performance as well. In addition, for 3DPCMs, the influence of pumpability and buildability on structural performance should also be considered. This section analyses the influence of these factors on the structural performance, which can potentially provide insights when designing 3DP concrete structures with desirable structure performance.

6.1 Pumpability and buildability

Good pumpability and buildability improve the structural performance of 3DPCMs. In contrast, the poor pumpability of the material increases the difficulty of pumping and hence brings a higher risk of discontinuity. Lack of steady and continuous material flow leads to defects such as tearing and variations of dimensions in the extruded layers, as shown in Fig. 13. In this situation, poor pumpability of material results in deteriorated structural performance. On the other hand, poor buildability of the material makes it difficult to reach the designed dimension of structures in one printing, as the structure may collapse during the printing process [63]. The continuous printing process may be suspended for the printed material to gain enough yield stress with time. As will be discussed in the later section, the long time gap between each printing impairs the interfacial bond of printed structure. Therefore, it is necessary to increase pumpability and buildability for better structural performance.



Fig. 13 Defects due to poor pumpability

6.2 Mechanical property

Due to the layer-by-layer deposition process, the printed structure has a distinctive orientation in manufacturing. The orientation further leads to the direction-dependent structural performance of 3D printed concrete structures, which is also referred to as anisotropic property [80]. The layer-by-layer 3D printing process introduces interfaces between adjacent layers, which potentially make its mechanical property less desirable compared with conventional concrete structures due to lack of adequate bond between printed layers. Cracks are more likely to initiate and propagate between adjacent printed layers with poor bonding. These cracks accelerate the penetration of detrimental substances into the structure, thus reducing its long-term load-carrying capacity. In addition, lack of bonding between layers may cause structure failure by shear force in horizontal loading cases, e.g. due to seismic loading.

Several experiments [81, 82] have been carried out to investigate the mechanical properties of 3DP structures. Through these experiments, it is found that 3D printed structures have distinctive anisotropic mechanical behavior. It is revealed that when the loading induces tension between the printed layers, the strength of the printed structure is greatly reduced. The highest strength is measured when the loading induces tension parallel to the printed layers.

Different from conventional cementitious materials, investigation on the mechanical strength of 3D printed cementitious materials at very early ages (e.g. several minutes to several hours) are highly valued.

Wolf et al. [29, 83] have reported the very early age mechanical properties of 3D printed cementitious materials. Evolution of compressive strength, Young's modulus and shear strength have been recorded through unconfined compressive tests and direct shear tests, which can be used to predict the elastic buckling or plastic collapse of the printed structure. The empirical Mohr-Coulomb model has been adopted to describe the evolution of shear strength, which is expressed as follows:

$$\tau_s = (0.058t + 3.05) + \sigma_n \tan(20^\circ) \quad (12)$$

where τ_s and σ_n are shear strength and compressive strength respectively.

There are several methods to potentially improve the bonding between adjacent printed layers. Le et al. [81] have confirmed that reducing printing time gap can effectively increase bonding strength. A similar conclusion has been reported by Panda et al. for 3D printed geopolymers concrete material [84]. Furthermore, the addition of fibers [85], adjustment of surface moisture level between layers [86] and bonding compound material such as latex [87] are also beneficial to interlayer bond strength.

Printing setup can affect printing quality and the consequent mechanical property of the printed structure. It is noticed that in the long 3D printing process, the printing quality gradually reduces with respect to time [81]. The gradual built-ups at the nozzle may affect the extrusion, leading to poorer printing quality [82]. It should also be taken into consideration that in some early printing system, the printed layers may not be able to come in full contact with each other due to nozzle outlet shape [81]. Defects may arise in the prints with poor morphology. However, the good prints could be made with circular nozzles or trapezoid nozzles [88].

6.3 Reinforcement

Concrete is a brittle material that is easy to generate cracks under tensile and/or flexural loading. To improve the structure ductility, reinforcement is introduced to form reinforced concrete structures as the conventional practice. In 3D cementitious material printing, introducing reinforcement in the printed structure is also necessary for engineering applications. The current practices of reinforcement in structures fabricated by 3D cementitious material printing can be classified into two general methods: (a) separate placement of reinforcement and cementitious material printing, and (b) simultaneous placement of reinforcement while printing. Both methods are proved effective for reinforcement entraining.

6.3.1 Separate placement of reinforcement and cementitious material printing

Early practices of 3D cementitious material printing adopt the first reinforcement entraining method, i.e. separate placement of reinforcement and cementitious material printing. In Concrete Printing technology developed by Lim et al. [14], the positions of steel reinforcement are reserved during cementitious material printing process. After the completion of the cementitious material printing, steel reinforcement will be placed inside. Complicated profiles can be obtained with the formation of composite structures [14] (see Fig. 14).



Fig. 14 Reinforcement in 3D printed structure by Concrete Printing ^[16]. Reproduced from Ref. [16] with permission from IAARC.

In Contour Crafting technology, the composite structures are produced through the printing of permanent formworks first, followed by the reinforcement placement and filling of other construction materials ^[89] (see Fig. 15). Reinforcing form ties are placed inside the printed permanent formwork. This characteristic offers flexibility in the structure design as the filling materials do not necessarily need to be the same as the printing materials. Functional construction materials, e.g., heat-insulating materials, self-compacting concrete can be conveniently introduced in this structure design without the need for additional formwork and/or support. The filling of construction material can even be skipped to form hollow structures if design permits.

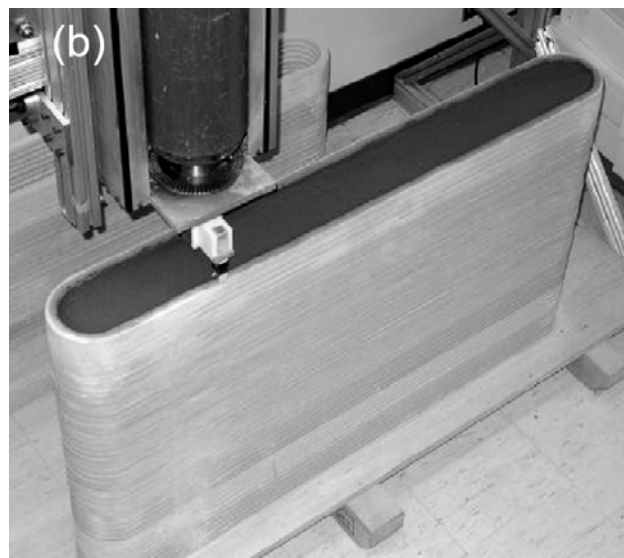
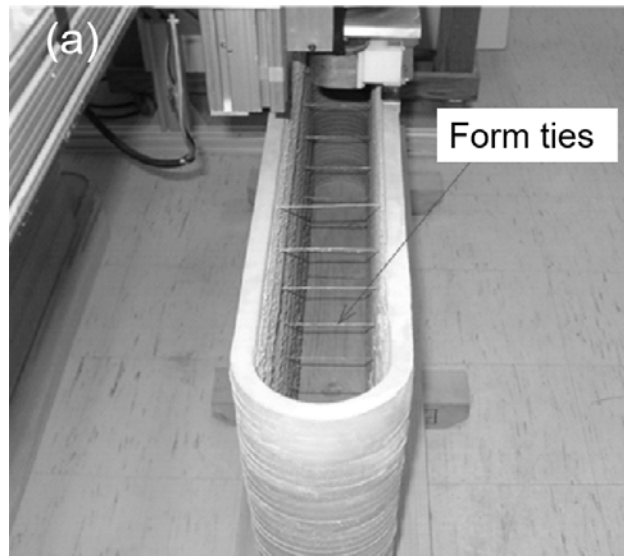


Fig. 15 Reinforcement in Contour Crafting ^[89]: (a) permanent formwork printed with inserted form ties; (b) A composite concrete wall made by Contour Crafting. Reproduced from Ref. [89] with permission © Inderscience.

Another practice of separate reinforcement placement and cementitious material printing is skeleton printing-spray technology ^[90]. ABS plastic or other printable plastic materials are used to print the reinforcement cage, which forms the skeleton of the desired structure. The cementitious material is sprayed afterwards, with the printed skeleton serving as the formwork and inner reinforcement. In this structure design, 3D printing offers the possibility to construct composite structures with different functional materials in vertical laminated layers ^[91]. The printed plastic reinforcements are easy to be duplicated and stacked in the skeleton printing-spraying system, which makes it possible to apply different construction materials with horizontal lamination. Lamination greatly increases varieties of structure design, which can be fully utilized to realize various functions.

There are also some reports for engineering applications adopting similar reinforcement entraining method. In the printing of wall structures by Winsun company, separate cementitious material printing

and placement of conventional steel reinforcement including longitudinal rebars and stirrups have been implemented [92]. In another engineering application by Huashang Tengda company, steel rebars are settled before cementitious material printing [93]. Special pipe and outlet have been developed in the project, where fresh cementitious material can be extruded to simultaneously form both sides of the wall and cover the settled steel rebars.

6.3.2 Simultaneous placement of reinforcement while printing

Instead of continuous reinforcement, short dispersed fibers can be introduced into the mix design of 3DPCMs to improve the structural performance. The fibers can be mixed with other raw ingredients and pumped to the nozzle for printing. Mechanical tests show that the introduction of glass fibers can effectively improve the flexural and compressive strength of the material while reducing flexural deflection [94, 95]. Alignment of fibers to the printing direction has been observed in the printed samples [95], which can further improve the structural performance.

Soltan and Li [96] have developed a self-reinforced cementitious composite for 3D printing by introducing short dispersed PVA fiber of 2% volume fraction. Due to the fiber alignment effect in 3D printing, printed coupons showed better mechanical properties compared with conventional cast ones. It is noteworthy that the printed coupons can reach nearly 3% tensile capacity, which is around 300 times that of conventional concrete materials [97]. Hence, the study further proves the effectiveness of this fiber reinforcing method in 3D printing.

A recently developed method is to entrain reinforcement while printing, which is shown in Fig. 16. The reinforcement can be cable wire or chain, which is entrained in each printed concrete layer [98]. Compared with the aforementioned methods, adoption of reinforcement entraining while printing reduces the total manufacturing time of reinforced structures. Pullout experiments show that the inserted cable wire has certain adhesive bonding with the matrix, although the ultimate pullout stress is lower compared with the inserted cables in casted samples (see Fig. 17).



Fig. 16 Reinforcement entraining while printing [98]. Reproduced from Ref. [98] with permission from MDPI.

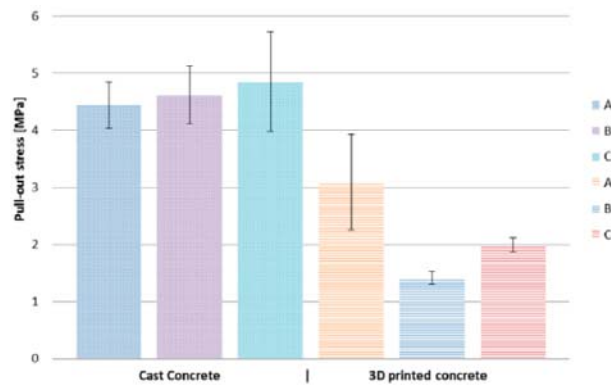


Fig. 17 Ultimate pullout stress for casted and 3D printed concrete specimens^[98]. Reproduced from Ref. [98] with permission from MDPI.

Bos et al.^{[98] [99]} conducted four-point bending tests to assess the mechanical performance of cable wire reinforced 3D printed filaments. Good post-cracking behaviors were observed in the cable wire reinforced filaments, including additional cracks and increased displacements under loading. Thus, the feasibility of this cable wire reinforcing method has been clarified. However, cable wires were placed in filaments parallel to the printing direction, which cannot penetrate the layer interface to strengthen interlayer bonding. Furthermore, large variation and limited post-cracking moment capacity due to slip of the wire and scatter of quality in printed filament were recorded. These issues need further exploration for the application of this method in 3D printing.

7. Conclusions

The article gives a systematical review of 3D printable cementitious materials (3DPCM). After the introduction of 3D cementitious material printing systems and corresponding printing process, the paper has proposed a multi-level material design (MMD) methodology for better review of the development of 3DPCM. MMD methodology is illustrated by three inter-connected pyramids, which represents three different levels in developing 3DPCM, i.e. mixture design, printing process and composite structure.

With the guidance of MMD, the three different levels of material design are reviewed successively. In the mixture design level, the influence of material composition on the rheological properties of 3DPCM is carefully examined. The effects of supplementary cementitious materials (SCM), superplasticizer and viscosity enhancing agent on rheological behavior are discussed. In the printing process level, pumpability and buildability of 3DPCM are illustrated and further correlated with rheological properties, tribological properties, delivery and placement of 3DPCM. The schematic diagram in relation to printing has been proposed to guide the tailoring of 3DPCM. In the composite structure level, the structure performance of 3DPCM is reviewed with the consideration of pumpability, buildability, mechanical property and reinforcement issue.

In general, the paper systematically reviews critical issues in developing 3DPCM. For a 3D printed concrete structure with desired structural performance, proper control of relevant parameters in the

mixture design and printing process should be employed when developing corresponding 3DPCMs. With the progress of material development in this field, more factors may be introduced in the aforementioned three levels. Nevertheless, MMD proposed in this paper can serve as a platform and be revised further to encompass further studies in this field.

Acknowledgement

This research is supported by the National Research Foundation, Prime Minister's Office, Singapore under its Medium-Sized Centre funding scheme, Singapore Centre for 3D Printing and Sembcorp Design & Construction Pte Ltd. The authors also would like to thank Prof Theo A. M. Salet from Department of the Built Environment, Eindhoven University of Technology, the Netherlands for very insightful discussions.

Reference

- [1] I. Gibson, D. Rosen, B. Stucker, Additive manufacturing technologies : 3D printing, rapid prototyping, and direct digital manufacturing, Springer, New York, U.S., 2015.
- [2] C.K. Chua, K.F. Leong, 3D Printing and Additive Manufacturing: Principles and Applications, World Scientific Publishing Co Inc, Singapore, 2017.
- [3] H. Kodama, A Scheme for Three-Dimensional Display by Automatic Fabrication of Three-Dimensional Model, IEICE Transactions on Electronics (Japanese Edition), 4 (1981) 237-241.
- [4] MIT Technology Review, 3D Printing Breaks the Glass Barrier, 2015.
- [5] E. Fantino, A. Chiappone, I. Roppolo, D. Manfredi, R. Bongiovanni, C.F. Pirri, F. Calignano, 3D Printing of Conductive Complex Structures with In Situ Generation of Silver Nanoparticles, Advanced Materials, 28 (2016) 3712-3717.
- [6] M. Qin, Y. Liu, J. He, L. Wang, Q. Lian, D. Li, Z. Jin, S. He, G. Li, Y. Liu, Z. Wang, Application of digital design and three-dimensional printing technique on individualized medical treatment, Chinese Journal of Reparative and Reconstructive Surgery, 28 (2014) 286-291.
- [7] Y.J. Seol, H.W. Kang, S.J. Lee, A. Atala, J.J. Yoo, Bioprinting technology and its applications, European Journal of Cardio-Thoracic Surgery, 46 (2014) 342-348.
- [8] J. Sun, W.B. Zhou, D.J. Huang, J.Y.H. Fuh, G.S. Hong, An Overview of 3D Printing Technologies for Food Fabrication, Food and Bioprocess Technology, 8 (2015) 1605-1615.
- [9] D. Weinstein, P. Nawara, Determining the Applicability of 3D Concrete Construction (Contour Crafting) of Low Income Houses in Select Countries, Cornell Real Estate Review, 13 (2015) 94-111.
- [10] T.A. Salet, Z.Y. Ahmed, F.P. Bos, H.L. Laagland, Design of a 3D printed concrete bridge by testing, Virtual and Physical Prototyping, (2018) 1-15.
- [11] D. Asprone, C. Menna, F.P. Bos, T.A. Salet, J. Mata-Falcón, W. Kaufmann, Rethinking reinforcement for digital fabrication with concrete, Cement and Concrete Research, (2018).
- [12] B. Khoshnevis, Automated construction by contour crafting—related robotics and information technologies, Automation in Construction, 13 (2004) 5-19.
- [13] D. Hwang, B. Khoshnevis, Concrete wall fabrication by contour crafting, The 21st International Symposium on Automation and Robotics in Construction (ISARC 2004), Jeju, South Korea, 2004.
- [14] S. Lim, R.A. Buswell, T.T. Le, S.A. Austin, A.G.F. Gibb, T. Thorpe, Developments in construction-

scale additive manufacturing processes, *Automation in Construction*, 21 (2012) 262-268.

[15] S. Lim, T.T. Le, J. Webster, R.A. Buswell, S.A. Austin, A.G.F. Gibb, T. Thorpe, Fabricating construction components using layered manufacturing technology, *Proceedings of Global Innovation in Construction Conference*, Loughborough, UK, 2009, pp. 512-520.

[16] S. Lim, R.A. Buswell, T.T. Le, R. Wackrow, S.A. Austin, A.G.F. Gibb, T. Thorpe, Development of a viable Concrete Printing process, *The 28th International Symposium on Automation and Robotics in Construction (ISARC 2011)*, Seoul, South Korea, 2011, pp. 665-670.

[17] F. Bos, R. Wolfs, Z. Ahmed, T. Salet, Additive manufacturing of concrete in construction: potentials and challenges of 3D concrete printing, *Virtual and Physical Prototyping*, 11 (2016) 209-225.

[18] C. Gosselin, R. Duballet, P. Roux, N. Gaudillière, J. Dirrenberger, P. Morel, Large-scale 3D printing of ultra-high performance concrete—a new processing route for architects and builders, *Materials and Design*, 100 (2016) 102-109.

[19] X. Zhang, M. Li, J.H. Lim, Y. Weng, Y.W.D. Tay, H. Pham, Q.-C. Pham, Large-scale 3D printing by a team of mobile robots, *Automation in Construction*, 95 (2018) 98-106.

[20] A. Kazemian, X. Yuan, E. Cochran, B. Khoshnevis, Cementitious materials for construction-scale 3D printing: Laboratory testing of fresh printing mixture, *Construction and Building Materials*, 145 (2017) 639-647.

[21] A. Pierre, D. Weger, A. Perrot, D. Lowke, Penetration of cement pastes into sand packings during 3D printing: analytical and experimental study, *Materials and Structures*, 51 (2018) 22.

[22] T. Wangler, Digital Concrete Processing: A Review, *The 1st International Conference on 3D Construction Printing (3DcP 2018)*, Melbourne, Australia, 2018, pp. 1-9.

[23] A.M. Neville, *Properties of concrete*, Prentice Hall/Pearson Education, Harlow, U.K. ; New York, U.S., 2002.

[24] Y. Weng, M. Li, M.J. Tan, S. Qian, Design 3D printing cementitious materials via Fuller Thompson theory and Marston-Percy model, *Construction and Building Materials*, 163 (2018) 600-610.

[25] Y. Weng, B. Lu, M.J. Tan, S. Qian, Rheology and Printability of Engineered Cementitious Composites-A Literature Review, *Proceedings of the 2nd International Conference on Progress in Additive Manufacturing*, Research Publishing Services, Singapore, 2016, pp. 427-432.

[26] Y.W. Tay, B. Panda, S.C. Paul, M.J. Tan, S. Qian, K.F. Leong, C.K. Chua, Processing and properties of construction materials for 3D printing, *Materials Science Forum*, Trans Tech Publications, Switzerland, 2016, pp. 177-181.

[27] H.A. Barnes, J.F. Hutton, K. Walters, *An introduction to rheology*, Elsevier, Amsterdam, Netherlands; New York, U.S., 1989.

[28] B. Panda, M. Li, Y.W. Tay, S.C. Paul, M.J. Tan, Modeling Fly Ash Based Geopolymer Flow for 3D Printing Applications, *International Conference on Advances in Construction Materials and Systems*, RILEM Publications, Chennai, India, 2017, pp. 9-16.

[29] R.J.M. Wolfs, F.P. Bos, T.A.M. Salet, Early age mechanical behaviour of 3D printed concrete: Numerical modelling and experimental testing, *Cement and Concrete Research*, 106 (2018) 103-116.

[30] Y. Qian, S. Kawashima, Flow onset of fresh mortars in rheometers: contribution of paste deflocculation and sand particle migration, *Cement and Concrete Research*, 90 (2016) 97-103.

[31] Y. Qian, S. Kawashima, Distinguishing dynamic and static yield stress of fresh cement mortars through thixotropy, *Cement and Concrete Composites*, 86 (2018) 288-296.

[32] S.A. Austin, P.J. Robins, C.I. Goodier, The rheological performance of wet-process sprayed mortars, *Mag Concrete Res*, 51 (1999) 341-352.

-
- [33] Y. Qian, S. Kawashima, Use of creep recovery protocol to measure static yield stress and structural rebuilding of fresh cement pastes, *Cement and Concrete Research*, 90 (2016) 73-79.
- [34] Q. Yuan, D. Zhou, B. Li, H. Huang, C. Shi, Effect of mineral admixtures on the structural build-up of cement paste, *Construction and Building Materials*, 160 (2018) 117-126.
- [35] S. Ma, Y. Qian, S. Kawashima, Experimental and modeling study on the non-linear structural build-up of fresh cement pastes incorporating viscosity modifying admixtures, *Cement and Concrete Research*, 108 (2018) 1-9.
- [36] A. Perrot, D. Rangeard, A. Pierre, Structural built-up of cement-based materials used for 3D-printing extrusion techniques, *Materials and Structures*, 49 (2016) 1213-1220.
- [37] S. Tang, X. Cai, Z. He, H. Shao, Z. Li, E. Chen, Hydration process of fly ash blended cement pastes by impedance measurement, *Construction and Building Materials*, 113 (2016) 939-950.
- [38] S. Tang, Z. Li, H. Shao, E. Chen, Characterization of early-age hydration process of cement pastes based on impedance measurement, *Construction and Building Materials*, 68 (2014) 491-500.
- [39] Y. Qian, K. Lesage, K. El Cheikh, G. De Schutter, Effect of polycarboxylate ether superplasticizer (PCE) on dynamic yield stress, thixotropy and flocculation state of fresh cement pastes in consideration of the Critical Micelle Concentration (CMC), *Cement and Concrete Research*, 107 (2018) 75-84.
- [40] P.F.G. Banfill, Rheological methods for assessing the flow properties of mortar and related materials, *Construction and Building Materials*, 8 (1994) 43-50.
- [41] B. Panda, S. Ruan, C. Unluer, M.J. Tan, Improving the 3D printability of high volume fly ash mixtures via the use of nano attapulgite clay, *Composites Part B: Engineering*, 165 (2019) 75-83.
- [42] D. Jiao, C. Shi, Q. Yuan, X. An, Y. Liu, H. Li, Effect of constituents on rheological properties of fresh concrete-A review, *Cement and Concrete Composites*, 83 (2017) 146-159.
- [43] C. Park, M. Noh, T. Park, Rheological properties of cementitious materials containing mineral admixtures, *Cement and Concrete Research*, 35 (2005) 842-849.
- [44] K. Khayat, A. Yahia, M. Sayed, Effect of supplementary cementitious materials on rheological properties, bleeding, and strength of structural grout, *ACI Materials Journal*, 105 (2008) 585-593.
- [45] P.-C. Nkinamubanzi, P.-C. Aïtcin, Cement and superplasticizer combinations: compatibility and robustness, *Cement, Concrete and Aggregates*, 26 (2004) 1-8.
- [46] V.S. Ramachandran, V. Malhotra, C. Jolicoeur, N. Spiratos, *Superplasticizers: properties and applications in concrete*, CANMET, Minister of Public Works and Government Services, Canada, 1998.
- [47] K.K. Yun, S.Y. Choi, J.H. Yeon, Effects of admixtures on the rheological properties of high-performance wet-mix shotcrete mixtures, *Construction and Building Materials*, 78 (2015) 194-202.
- [48] R. Flatt, I. Schöber, *Superplasticizers and the rheology of concrete*, Understanding the rheology of concrete, Elsevier, 2012, pp. 144-208.
- [49] Y. Qian, G. De Schutter, Different Effects of NSF and PCE Superplasticizer on Adsorption, Dynamic Yield Stress and Thixotropy of Cement Pastes, *Materials*, 11 (2018).
- [50] G. Gelardi, *Characterization of Comb Copolymer Superplasticizers by a Multi-Technique Approach*, ETH Zurich, 2017.
- [51] K.H. Khayat, Viscosity-enhancing admixtures for cement-based materials—an overview, *Cement and Concrete Composites*, 20 (1998) 171-188.
- [52] R. Bouras, A. Kaci, M. Chaouche, Influence of viscosity modifying admixtures on the rheological behavior of cement and mortar pastes, *Korea-Australia Rheology Journal*, 24 (2012) 35-44.
- [53] A. Leemann, F. Winnefeld, The effect of viscosity modifying agents on mortar and concrete, *Cement and Concrete Composites*, 29 (2007) 341-349.

-
- [54] Y. Zhang, Y. Zhang, G. Liu, Y. Yang, M. Wu, B. Pang, Fresh properties of a novel 3D printing concrete ink, *Construction and Building Materials*, 174 (2018) 263-271.
- [55] T. Voigt, J.-J. Mbele, K. Wang, S.P. Shah, Using fly ash, clay, and fibers for simultaneous improvement of concrete green strength and consolidability for slip-form pavement, *Journal of Materials in Civil Engineering*, 22 (2010) 196-206.
- [56] Y. Qian, G. De Schutter, Enhancing thixotropy of fresh cement paste with nanoclay in presence of polycarboxylate ether superplasticizer (PCE), *Cement and Concrete Research*, 111 (2018) 15-22.
- [57] H. Yamaguchi, *Engineering fluid mechanics*, Springer Science & Business Media, 2008.
- [58] R.P. Chhabra, J.F. Richardson, *Non-Newtonian flow and applied rheology : engineering applications*, Butterworth-Heinemann/Elsevier, Amsterdam, Netherlands ; Boston, U.S., 2008.
- [59] D. Kaplan, *Pompage des bétons*, École nationale des ponts et chaussées, Marne-la-Vallée, France, 2000 (In French).
- [60] G.R. Lomboy, K. Wang, P. Taylor, S.P. Shah, Guidelines for design, testing, production and construction of semi-flowable SCC for slip-form paving, *International Journal of Pavement Engineering*, 13 (2012) 216-225.
- [61] H. Hoornahad, *Toward Development of Self-Compacting No-Slump Concrete Mixtures*, Delft University of Technology, Delft, the Netherlands, 2014.
- [62] B. Khoshnevis, X. YUAN, B. Zahiri, J. Zhang, B. Xia, Deformation Analysis of Sulfur Concrete Structures Made by Contour Crafting, *AIAA SPACE 2015 Conference and Exposition*, 2015, pp. 4452.
- [63] T.T. Le, S.A. Austin, S. Lim, R.A. Buswell, A.G.F. Gibb, T. Thorpe, Mix design and fresh properties for high-performance printing concrete, *Materials and Structures*, 45 (2012) 1221-1232.
- [64] K.-H. Jeon, M.-B. Park, M.-K. Kang, J.-H. Kim, Development of an automated freeform construction system and its construction materials, *Proceedings of the 30th International Symposium on Automation and Robotics in Construction (ISARC 2013)*, Montreal, Canada, 2013, pp. 1359-1365.
- [65] G. Ma, Z. Li, L. Wang, Printable properties of cementitious material containing copper tailings for extrusion based 3D printing, *Construction and Building Materials*, 162 (2018) 613-627.
- [66] R.S. Ahari, T.K. Erdem, K. Ramyar, Time-dependent rheological characteristics of self-consolidating concrete containing various mineral admixtures, *Construction and Building Materials*, 88 (2015) 134-142.
- [67] N. Khalil, G. Aouad, K. El Cheikh, S. Rémond, Use of calcium sulfoaluminate cements for setting control of 3D-printing mortars, *Construction and Building Materials*, 157 (2017) 382-391.
- [68] Y.Y. Kim, H.J. Kong, V.C. Li, Design of engineered cementitious composite suitable for wet-mixture shotcreting, *ACI Materials Journal*, 100 (2003) 511-518.
- [69] Y.C. Fu, X.P. Cao, Z.J. Li, Printability of Magnesium Potassium Phosphate Cement with Different Mixing Proportion for Repairing Concrete Structures in Severe Environment, *Key Engineering Materials*, 711 (2016) 989-995.
- [70] J.P. Won, U.J. Hwang, C.K. Kim, S.J. Lee, Mechanical performance of shotcrete made with a high-strength cement-based mineral accelerator, *Construction and Building Materials*, 49 (2013) 175-183.
- [71] T. Binns, Pumped concrete, in: B.S. Choo (Ed.) *Advanced Concrete Technology*, Butterworth-Heinemann, Oxford, U.K., 2003, pp. 1-33.
- [72] E. Kempster, Pumpable concrete, in: *Building Research Station (Ed.) Garston, U.K.*, 1968.
- [73] J. Assaad, K.H. Khayat, J. Daczko, Evaluation of static stability of self-consolidating concrete, *ACI Materials Journal*, 101 (2004) 207-215.
- [74] A. Johansson, K. Tuutti, *Pumped concrete and pumping of concrete*, 1976.

[75] S.J. Keating, J.C. Leland, L. Cai, N. Oxman, Toward site-specific and self-sufficient robotic fabrication on architectural scales, *Science Robotics*, 2 (2017).

[76] D. Beaupre, Rheology of high performance shotcrete, University of British Columbia, Vancouver, Canada, 1994.

[77] M. Jolin, D. Beaupre, Understanding wet-mix shotcrete: mix design, specifications, and placement, *Surface Support Liners* 2003, Quebec City, Canada, 2003, pp. 6-12.

[78] A. Suiker, Mechanical performance of wall structures in 3D printing processes: theory, design tools and experiments, *International Journal of Mechanical Sciences*, 137 (2018) 145-170.

[79] J. Young, WinSun 3D Prints Build Garden Villas in Suzhou Within One Week, 2016.

[80] B. Lu, M.J. Tan, S. Qian, A Review of 3D Printable Construction Materials and Applications, *Proceedings of the 2nd International Conference on Progress in Additive Manufacturing*, Research Publishing Services, Singapore, 2016, pp. 330-335.

[81] T.T. Le, S.A. Austin, S. Lim, R.A. Buswell, R. Law, A.G.F. Gibb, T. Thorpe, Hardened properties of high-performance printing concrete, *Cement and Concrete Research*, 42 (2012) 558-566.

[82] P. Feng, X. Meng, J.-F. Chen, L. Ye, Mechanical properties of structures 3D printed with cementitious powders, *Construction and Building Materials*, 93 (2015) 486-497.

[83] R. Wolfs, F. Bos, T. Salet, Correlation between destructive compression tests and non-destructive ultrasonic measurements on early age 3D printed concrete, *Construction and Building Materials*, 181 (2018) 447-454.

[84] B. Panda, S.C. Paul, N.A.N. Mohamed, Y.W.D. Tay, M.J. Tan, Measurement of tensile bond strength of 3D printed geopolymers mortar, *Measurement*, 113 (2018) 108-116.

[85] S. Christ, M. Schnabel, E. Vorndran, J. Groll, U. Gbureck, Fiber reinforcement during 3D printing, *Materials Letters*, 139 (2015) 165-168.

[86] J.G. Sanjayan, B. Nematollahi, M. Xia, T. Marchment, Effect of surface moisture on inter-layer strength of 3D printed concrete, *Construction and Building Materials*, 172 (2018) 468-475.

[87] Q. Zhang, V.C. Li, Development of durable spray-applied fire-resistive Engineered Cementitious Composites (SFR-ECC), *Cement & Concrete Composites*, 60 (2015) 10-16.

[88] W. Lao, M. Li, L. Masia, M.J. Tan, Approaching Rectangular Extrudate in 3D Printing for Building and Construction by Experimental Iteration of Nozzle Design, *Proceedings of Solid Freeform Fabrication Symposium*, Austin, TX, U.S., 2017, pp. 2612-2623.

[89] B. Khoshnevis, D. Hwang, K.-T. Yao, Z. Yeh, Mega-scale fabrication by contour crafting, *International Journal of Industrial and Systems Engineering*, 1 (2006) 301-320.

[90] Architect Magazine, This Architect-Designed Wall System Has a 3D-Printed Core, 2015.

[91] W. Gao, Y.B. Zhang, D. Ramanujan, K. Ramani, Y. Chen, C.B. Williams, C.C.L. Wang, Y.C. Shin, S. Zhang, P.D. Zavattieri, The status, challenges, and future of additive manufacturing in engineering, *Computer-Aided Design*, 69 (2015) 65-89.

[92] Sculpteo, 3D printing construction & architecture: building the home of the future, 2015.

[93] engineering.com, 400-Square-Meter Villa 3D Printed Onsite in Just 45 Days, 2016.

[94] B. Panda, S.C. Paul, M.J. Tan, Anisotropic mechanical performance of 3D printed fiber reinforced sustainable construction material, *Materials Letters*, 209 (2017) 146-149.

[95] M. Hambach, D. Volkmer, Properties of 3D-printed fiber-reinforced Portland cement paste, *Cement and Concrete Composites*, 79 (2017) 62-70.

[96] D.G. Soltan, V.C. Li, A self-reinforced cementitious composite for building-scale 3D printing, *Cement and Concrete Composites*, (2018).

968 [97] V.C. Li, On engineered cementitious composites (ECC), Journal of Advanced Concrete Technology,
969 1 (2003) 215-230.
970 [98] F.P. Bos, Z.Y. Ahmed, E.R. Jutinov, T.A.M. Salet, Experimental Exploration of Metal Cable as
971 Reinforcement in 3D Printed Concrete, Materials, 10 (2017) 1314.
972 [99] F.P. Bos, Z.Y. Ahmed, R.J.M. Wolfs, T.A.M. Salet, 3D Printing Concrete with Reinforcement,
973 High Tech Concrete: Where Technology and Engineering Meet, Springer, 2018, pp. 2484-2493.
974